Pergamon

Int. J. Solids Structures Vol. 31, No. 6, pp. 835–848, 1994

0020–7683/94 $6.00 + .00

EFFECTS OF SUPPORT CONFIGURATION ON THE PARAMETRIC EXCITATION OF A PLATE

H. P. LEE and T. Y. NG
Department of Mechanical and Production Engineering, National University of Singapore, 10 Kent Ridge Crescent, Singapore 0511, Republic of Singapore

(*Received* 9 *February* 1993; *in revised form* 9 *September* 1993)

Abstract—The equations of motions of a classical thin plate moving over multiple supports are formulated based on Hamilton's principle and the assumed mode method. The supports are frictionless line supports spanning the entire or partial width of the plate with the plate being pushed or pulled over them. A feature of the present formulation is that its complexity does not increase with increased number of line supports. The effects of support length and eccentricity in the locations of the support are examined for various prescribed longitudinal excitations of the plate.

1. INTRODUCTION

Many studies have been reported for the parametric excitation of beams and beam systems. Beal (1965) presented the stability analysis of a flexible missile, modeled as a slender beam, under constant and pulsating thrusts. Storch and Gate (1985) analysed a free–free beam undergoing axial acceleration. Nayfeh and Mook (1979) gave a comprehensive summary of past research through 1979. The dynamics of a beam of finite length moving over supports, related to the dynamics of prismatic joints in robots, was first presented by Buffinton and Kane (1985) using Kane's dynamics and subsequently by Buffinton (1990, 1992) in related works. As pointed out in these works, the forces exerted on the beam by the supports have magnitudes depending on the motion of the beam. Moreover, the beam moves not only relative to an inertial frame but also relative to its support. Lee (1993) presented an alternative formulation based on Hamilton's principle and the assumed mode method for studying the dynamic responses of a beam moving over multiple supports. The external forces that caused the motion of the beam were either in the form of frictional forces supplied by a roller which acted as a support at the same time, or external forces applied at one end of the beam. Numerical simulations showed that the behaviors of a beam with these two different modes of applied forces could be dramatically different depending on the frequency of the prescribed longitudinal excitation.

The dynamics of plates subjected to a moving load have been treated in the book by Frýba (1972). A list of early works was appended at the end of the book. Other studies taking into account the effects of moving masses, non-uniform thickness, and elastic foundation were presented by Raske and Schlack (1967), Stanisic *et al.* (1968), Wu *et al.* (1987), and Gbadeyan and Oni (1992). A related problem of a plate executing small motions relative to a reference frame undergoing large overall rigid body motion was presented by Banerjee and Kane (1989). Other works on the dynamics of moving or rotating plates, for example, Leissa and Co (1984), Young and Liou (1992), were related to the vibration of cantilever plates which were often used as models for rotating blades in turbomachinery. The present problem of a plate subject to longitudinal excitation over multiple line supports has not been analysed.

2. THEORY AND FORMULATIONS

The plate considered is assumed to be a thin, uniform plate of dimension $l \times w$ moving horizontally over two line supports. The first support configuration to be considered consists of two line supports located at $x = s_1$ and $x = s_2$ spanning the width w of the plate shown in Fig. 1. The remaining support configurations to be considered can be described by two

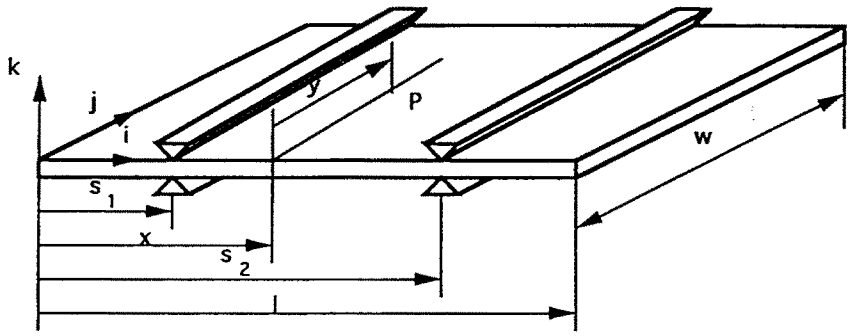

Fig. 1. A plate moving over two frictionless line supports spanning the width of the plate.

line supports spanning different portions of the plate as shown in Fig. 2. The lengths of the two line supports located at $x = s_1$ and $x = s_2$ are, respectively, $b_2 - b_1$ and $c_2 - c_1$. Horizontal forces are applied at the left edge of the plate to pull or push the plate over these line supports. The assumptions made in the following formulation are that transverse deflections are small so that the dynamic behavior of the plate is governed by classical thin plate theory. A set of mutually perpendicular unit vectors **i**, **j**, and **k** is assumed to be fixed in the plate. Flexibility of the plate in the two in-plane directions **i** and **j** is assumed to be negligible compared to the lateral direction **k**.

The position vector of a general point P on the deformed plate is given by

$$\mathbf{p} = x\mathbf{i} + y\mathbf{j} + u(x, y, t)\mathbf{k}, \tag{1}$$

where u, a function of x, y, and t, is the transverse deflection of the plate. It should be noted that the variables x, y, and u measure displacements along three inertially fixed axes coincident with **i**, **j**, and **k** for an undeformed plate. Therefore, the measurements x, y, and u are not directed in the **i**, **j**, and **k** direction for the deformed plate. Equation (1) consequently represents a linearized description of the displacements of a point on the plate.

The velocity at the point is

$$\mathbf{v}_p = U\mathbf{i} + \dot{u}\mathbf{k} \tag{2}$$

where $\dot{u} = (\mathrm{d}u/\mathrm{d}t)$ and $U\mathbf{i}$ is the prescribed velocity of the plate at $x = 0$ as a result of the external applied forces at the left edge of the plate. Due to the assumption of in-plane rigidity, U is also the **i** component of the velocity for every point on the plate.

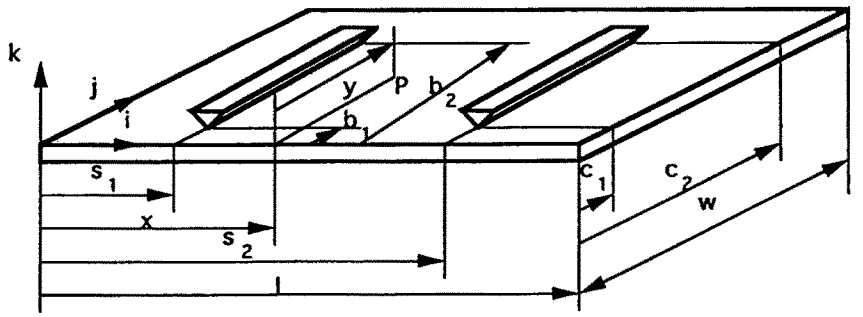

Fig. 2. A plate moving over two frictionless line supports partially spanning the width of the plate.

The kinetic energy T of the plate is

$$T = \tfrac{1}{2}m\int_0^w \int_0^l (U^2+\dot{u}^2)\,dx\,dy, \tag{3}$$

where m is the mass of the plate per unit area.

Assuming classical thin plate theory, the elastic strain energy of the plate due to bending is

$$V_\varepsilon = \frac{1}{2}\int_0^w \int_0^l D\left[\left(\frac{\partial^2 u}{\partial x^2}\right)^2 + \left(\frac{\partial^2 u}{\partial y^2}\right)^2 + 2\nu\frac{\partial^2 u}{\partial x^2}\frac{\partial^2 u}{\partial y^2} + 2(1-\nu)\left(\frac{\partial^2 u}{\partial x \partial y}\right)^2\right]dx\,dy, \tag{4}$$

where D and ν are the flexural rigidity and the Poisson's ratio of the plate.

The line supports are regarded to be very stiff line springs of stiffness k. The potential energy due to the line supports for the support configuration shown in Fig. 2 is

$$V_s = \tfrac{1}{2}k\int_{b_1}^{b_2} u^2(s_1,y)\,dy + \tfrac{1}{2}k\int_{c_1}^{c_2} u^2(s_2,y)\,dy, \tag{5}$$

where $x = s_1$ and $x = s_2$ are the coordinates of the line supports relative to the moving plate. These relative locations of the line supports change with the motion of the plate. The quantities $u(s_1, y)$ and $u(s_2, y)$ are the deflections of the plate at $x = s_1$ and $x = s_2$, respectively. It can be seen from the above expression that increasing the number of line supports will only increase the number of terms in eqn (5). It will not directly affect the expressions for kinetic energy, strain energy, and the following expression for the potential energy due to the axial forces of the plate. However, increasing the number of line supports does affect the number of modal functions, to be presented subsequently, and the computation time needed to calculate a solution of a given accuracy.

The expression given by eqn (5) is also applicable to the support configuration shown in Fig. 1 by equating $b_1 = c_1 = 0$ and $b_2 = c_2 = w$.

The potential energy due to the in-plane forces per unit width, f_x, in the **i** direction caused by the motion of the plate is

$$V_a = \frac{1}{2}\int_0^w \int_0^l f_x\left(\frac{\partial u}{\partial x}\right)^2 dx\,dy. \tag{6}$$

For a plate moving over the pair of frictionless line supports shown in Figs 1 and Fig. 2, the right edge of the plate is stress free as the plate is being pulled or pushed over the line supports by external forces applied at the left edge of the plate. The in-plane forces per unit width in the **i** direction for the remaining part of the plate are:

$$\begin{aligned} f_x &= -m\int_x^l \dot{U}\,dr, \\ &= -m\dot{U}(l-x). \end{aligned} \tag{7}$$

Using the assumed mode method, the quantity u can be expressed as

$$u = \sum_{n=1}^{N} q_n(t)\phi_n(x,y), \tag{8}$$

where ϕ_n are shape functions that satisfy the geometric boundary conditions at the four edges of the plate. For the present study, ϕ_n are assumed to be products of the normalized

modal functions for the vibration of a uniform unrestrained beam. The assumed functions are:

$$\phi_n(x,y) = \psi_i(x)\varphi_j(y). \tag{9}$$

The shape functions $\psi_i(x)$ and $\varphi_j(y)$ are defined as

$$\psi_1(x) = 1, \tag{10}$$

$$\psi_2(x) = \sqrt{3}\left(1-\frac{2x}{l}\right), \tag{11}$$

$$\psi_i(x) = \cos\frac{\lambda_{i-2}x}{l} + \cosh\frac{\lambda_{i-2}x}{l} - \gamma_{i-2}\left(\sin\frac{\lambda_{i-2}x}{l} + \sinh\frac{\lambda_{i-2}x}{l}\right) \quad (i = 3,\ldots,I), \tag{12}$$

$$\varphi_1(y) = 1, \tag{13}$$

$$\varphi_2(y) = \sqrt{3}\left(1-\frac{2y}{w}\right), \tag{14}$$

$$\varphi_j(y) = \cos\frac{\lambda_{j-2}y}{w} + \cosh\frac{\lambda_{i-2}y}{w} - \gamma_{j-2}\left(\sin\frac{\lambda_{j-2}y}{w} + \sinh\frac{\lambda_{j-2}y}{w}\right) \quad (j = 3,\ldots,J), \tag{15}$$

where

$$\gamma_p = \frac{\cos\lambda_p - \cosh\lambda_p}{\sin\lambda_p - \sinh\lambda_p}, \tag{16}$$

for $p = i$ or j and $\lambda_1, \ldots, \lambda_I$ or λ_J are the consecutive roots of the transcendental equation

$$1 - \cos\lambda\cosh\lambda = 0. \tag{17}$$

The functions ψ_1 and φ_1 correspond to the rigid body translation of an unrestrained beam whereas ψ_2 and φ_2 are the shape functions for rigid body rotation. The total number of terms in the assumed form of u is $N = I \times J$. In the following formulation, I is made to be equal to J. The functions ϕ_n are defined as:

$$\phi_n(x,y) = \psi_n(x)\varphi_1(y) \qquad \text{for } n = 1,\ldots,I, \tag{18}$$

$$\phi_n(x,y) = \psi_{n-I}(x)\varphi_2(y) \qquad \text{for } n = I+1,\ldots,2I, \tag{19}$$

$$\vdots = \vdots$$

$$\phi_n(x,y) = \psi_{n-(I-1)I}(x)\varphi_1(y) \quad \text{for } n = (I-1)I+1,\ldots,I^2. \tag{20}$$

The assumed form of u enables the kinetic energy, the strain energy, and the potential energy to be expressed in matrix form as follows:

$$T = \tfrac{1}{2}m\dot{\mathbf{q}}^T\mathbf{H}\dot{\mathbf{q}}, \tag{21}$$

$$V_\varepsilon = \tfrac{1}{2}D\mathbf{q}^T\mathbf{M}\mathbf{q}, \tag{22}$$

$$V_s = \tfrac{1}{2}k\mathbf{q}^T(\boldsymbol{\Phi}_1 + \boldsymbol{\Phi}_2)\mathbf{q} \tag{23}$$

$$= \tfrac{1}{2}k\mathbf{q}^T\boldsymbol{\Phi}\mathbf{q},$$

$$V_a = \tfrac{1}{2}m\dot{U}\mathbf{q}^T\mathbf{Y}\mathbf{q}, \tag{24}$$

where $\mathbf{H}$, $\mathbf{M}$, $\mathbf{Y}$, $\mathbf{Q}$, $\boldsymbol{\Phi}_1$, and $\boldsymbol{\Phi}_2$ are matrices defined as:

$$(\mathbf{H})_{ij} = \int_0^w \int_0^l \phi_i \phi_j \, dx \, dy, \tag{25}$$

$$(\mathbf{M})_{ij} = \int_0^w \int_0^l \left(\frac{\partial^2 \phi_i}{\partial x^2} \frac{\partial^2 \phi_j}{\partial x^2} + \frac{\partial^2 \phi_i}{\partial y^2} \frac{\partial^2 \phi_j}{\partial y^2} + \nu \frac{\partial^2 \phi_i}{\partial x^2} \frac{\partial^2 \phi_j}{\partial y^2} + \nu \frac{\partial^2 \phi_j}{\partial x^2} \frac{\partial^2 \phi_i}{\partial y^2} + 2(1-\nu) \frac{\partial^2 \phi_i}{\partial x \partial y} \frac{\partial^2 \phi_j}{\partial x \partial y} \right) dx \, dy, \tag{26}$$

$$(\mathbf{Y})_{ij} = \int_0^w \int_0^l -(l-x) \frac{\partial \phi_i}{\partial x} \frac{\partial \phi_j}{\partial x} \, dx \, dy, \tag{27}$$

$$(\mathbf{\Phi}_1)_{ij} = \int_{b_1}^{b_2} \phi_i(x = s_1, y) \phi_j(x = s_1, y) \, dy, \tag{28}$$

$$(\mathbf{\Phi}_2)_{ij} = \int_{c_1}^{c_2} \phi_i(x = s_2, y) \phi_j(x = s_2, y) \, dy. \tag{29}$$

The matrices **M**, **H**, **Y**, $\mathbf{\Phi}_1$, and $\mathbf{\Phi}_2$ are symmetric. All the matrices except $\mathbf{\Phi}_1$ and $\mathbf{\Phi}_2$ are independent of time. The matrices $\mathbf{\Phi}_1$ and $\mathbf{\Phi}_2$ need to be updated as the plate is moving over the supports. The quantities $\mathbf{q}$ and $\dot{\mathbf{q}}$ are $n \times 1$ column vectors consisting of q_i and $\dot{q}_i$, respectively.

The Lagrangian of the plate involving u can be expressed as

$$\mathscr{L} = T - V_\varepsilon - V_\alpha - V_s. \tag{30}$$

By making use of Hamilton's principle, the Euler–Lagrange equation for a plate moving over line supports is determined to be:

$$m\mathbf{H}\ddot{\mathbf{q}} + (D\mathbf{M} + m\dot{U}\mathbf{Y} + k\mathbf{\Phi})\mathbf{q} = 0. \tag{31}$$

These equations of motion are incorporated into numerical simulation programs for investigating the response of a plate undergoing various prescribed longitudinal excitations. The numerical integrations are performed using the fourth order Runge–Kutta method.

3. RESULTS AND SIMULATIONS

For the present numerical simulations, $l = w = 1$ m, $m = 1$ kg m^{-2}, and $D = 1$ N-m. The plate is assumed to be moving over two line supports with a separation of $s_2 - s_1 = 0.25$ m. The initial configuration of the plate is such that the two supports are located symmetrically at $s_1 = 0.375$ m and $s_2 = 0.625$ m. The initial shape of the plate is described by

$$u = \psi_1(x)\varphi_1(y)q_1(0) + \psi_3(x)\varphi_1(y)q_3(0). \tag{32}$$

The initial values of q_1 and q_3 are determined from the conditions that $u = 0$ m for both supports at $s_1 = 0.375$ m and $s_2 = 0.625$ m, and $u = 0.01$ m at $x = 0$ m and at $x = l$ m. Since ϕ_1 and ψ_1 correspond to the rigid body translation for a beam, and ψ_3 is the first flexural mode for a beam, the initial shape of the plate is the first symmetric flexural mode shape of an unrestrained beam in the x direction passing through the two supports. The natural frequencies for this plate with the two line supports without longitudinal motion are 15.864, 24.163, 45.229, 48.650, and 59.515 rad s^{-1} for the first five modes.

For a prescribed longitudinal sinusoidal excitation of the plate, the variation of s_1 is assumed to be

$$s_1 = 0.375 - A \sin \Omega t \text{ (m)}. \tag{33}$$

For a plate moving over supports shown in Fig. 1 with the line supports spanning the width of the plate, the transverse displacements at $x = 0$ and $y = 0.5$ m of the plate for $\Omega = 20$ rad/sec and $A = 0.05$ are shown in Fig. 3 using a 25-term approximation for u ($N = 25$, $I = J = 5$). It can be seen that the point displacements at $x = 0$ and $y = 0.5$ m for $k = 10^5$ and $k = 5 \times 10^4$ N m^{-1} per unit length of support are almost identical. On the other hand, the displacements at the left support ($x = s_1$) are almost negligible for $k = 10^5$ N m^{-1} per unit length of support compared with the corresponding point displacements at the edge. The displacements at the right support ($x = s_2$) are also found to be negligible for this assumed value of stiffness for the line support. The execution time for the numerical integrations is found to increase with increased value of k. For the following simulations, k is chosen to be 10^5 N/m per unit length of support. Numerical simulations for such a value of k can be performed quite efficiently within a few minutes, depending on the prescribed longitudinal excitation, on a 486-50 MHz personal computer. Numerical results for a convergence study with respect to the number of terms (N) for u is presented in Fig. 4 for $\Omega = 20$ rad/sec, $A = 0.05$, and $k = 10^5$ N/m per unit length of line support. It can be seen that the point displacements at $x = 0$ and $y = 0.5$ m for $N = 25$ with $I = J = 5$ and $N = 16$ with $I = J = 4$ are almost identical. Consequently, a 25-term approximation for u with $I = J = 5$ is used for the following numerical simulations.

The point displacements for three different points on the left edge of the plate for $\Omega = 20$, 30, 32, and 34 rad s^{-1} and $A = 0.05$ are shown in Fig. 5. The point displacements for the three points on the left edge are found to be identical as the initial shape of the plate is assumed to be consisting of only the first rigid body translation mode in the **j** direction [$\varphi_1(y)$] as shown in eqn (32). Numerical simulations show that the subsequent expression for u comprises mainly terms which are products of $\varphi_1(y)$ and all of the assumed functions for $\psi_i(x)$. Contributions from terms involving $\varphi_2(y)$ to $\varphi_5(y)$ appear to be null or negligible probably due to rounding errors in the numerical integrations. The plate shows a stable behavior for $\Omega = 20$ and 30 rad/sec. However, at $\Omega = 32$ rad s^{-1}, an unstable behavior in

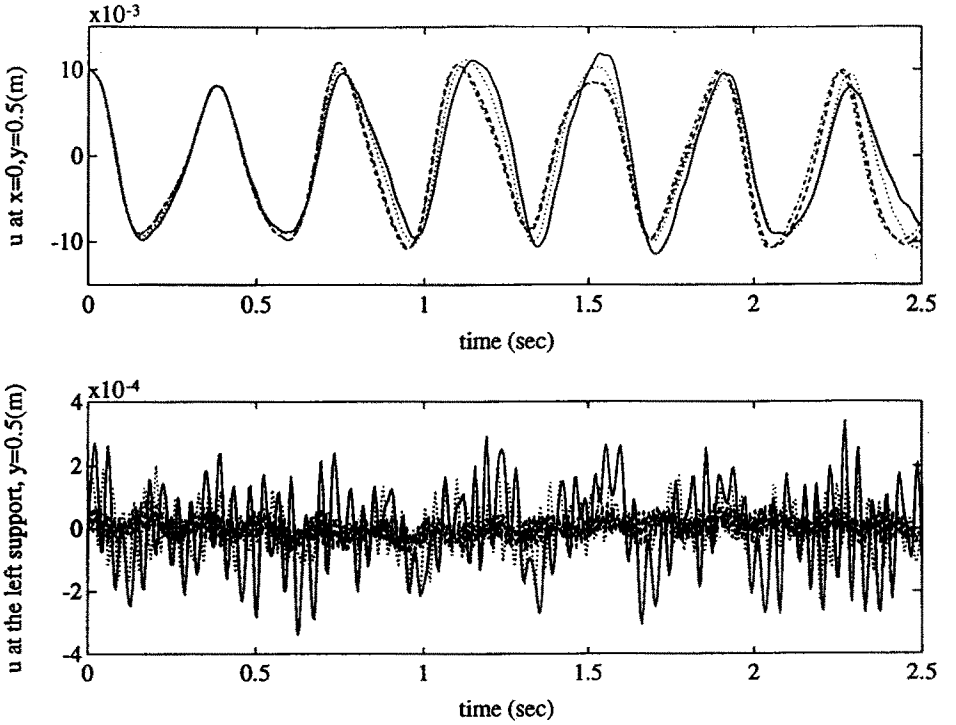

Fig. 3. Point displacements at the left edge of the plate and at the left support. $k = 5 \times 10^3$ N/m, ———; $k = 1 \times 10^4$ N/m, ···; $k = 5 \times 10^4$ N/m, - - -; $k = 1 \times 10^5$ N/m, - · - · -; for a unit length of line support.

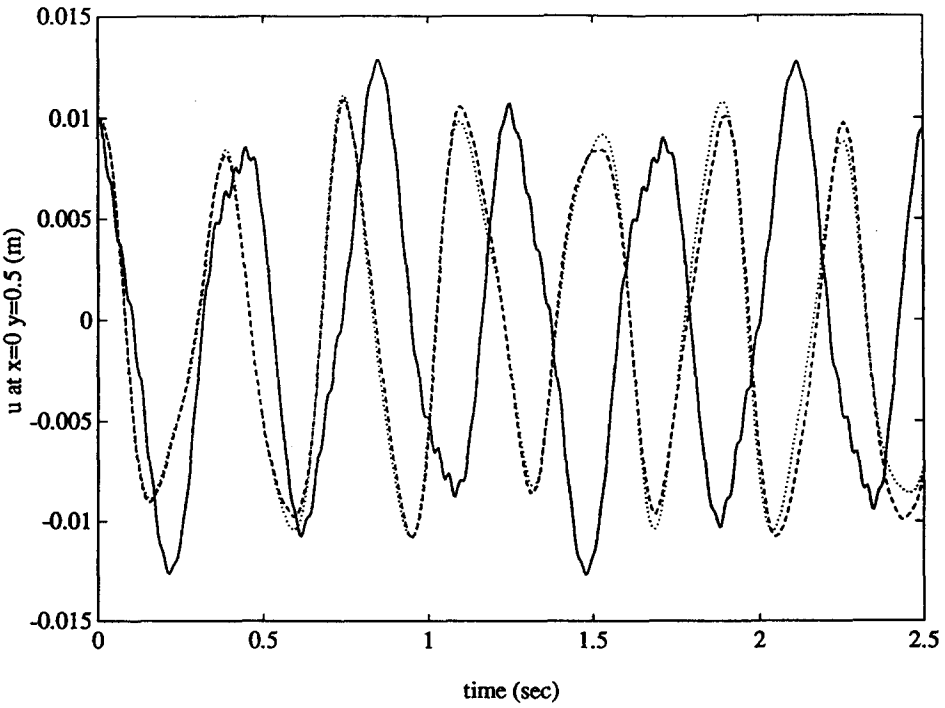

Fig. 4. Point displacements at the left edge of the plate. $N = 9, I = J = 3$, ———; $N = 16, I = J = 4$, ···; $N = 25, I = J = 5$, - - -.

the form of an exponential increase of the amplitude vibration is observed. The unstable region in terms of Ω appears to be narrow as the stability is restored when Ω is increased to 34 rad s^{-1}. Other regions of instability were also observed for different values of Ω.

To study the effect of initial prescribed shape of the plate on the stability behavior, the initial shape of the plate is changed to:

$$u = \psi_1(x)\varphi_3(y)q_{11}(0) + \psi_3(x)\varphi_3(y)q_{13}(0). \tag{34}$$

The initial values of q_{11} and q_{13} are determined from the conditions that $u = 0$ m for both supports at $s_1 = 0.375$ m and $s_2 = 0.625$ m, and $u = 0.01$ m at $x = 0$ m and at $x = l$ m at the four corners of the plate.

The assumed function in the **j** direction is the first flexural mode for a beam. Numerical results in Fig. 6 show that the stability behaviors of the plate are the same as the plate with stability behaviors presented in Fig. 5, consistent with the fact that the stability due to the parametric excitation of a plate is not dependent on initial conditions. Once again for the present case of a plate with supports spanning the width of the plate, numerical simulations show that the subsequent expression for u only involves terms which are products of $\varphi_3(y)$ and all of the assumed functions for $\psi_i(x)$. Terms involving $\varphi_1(y)$, $\varphi_2(y)$, $\varphi_4(y)$ and $\varphi_5(y)$, which do not appear in the initial prescribed function for u, appear to have null or negligible contribution in the subsequent expression for u. Consequently, the point displacements at the two left-hand corners of the plate appear to be identical when the results shown in Fig. 6 are magnified in scale.

A general stability analysis can be performed by the method presented by Buffinton and Kane (1985) using Floquet's theory. Such a laborious analysis will not be performed for the present study. The present study, however, will attempt to show the different behavior of the plate when the support configuration is varied.

For a plate shown in Fig. 2 with symmetrically located line supports which span only the central portion of the plate with $b_1 = c_1 = 0.25$ m and $b_2 = c_2 = 0.75$ m, numerical results corresponding to the two initial shapes of the plate described by eqns (32) and (34),

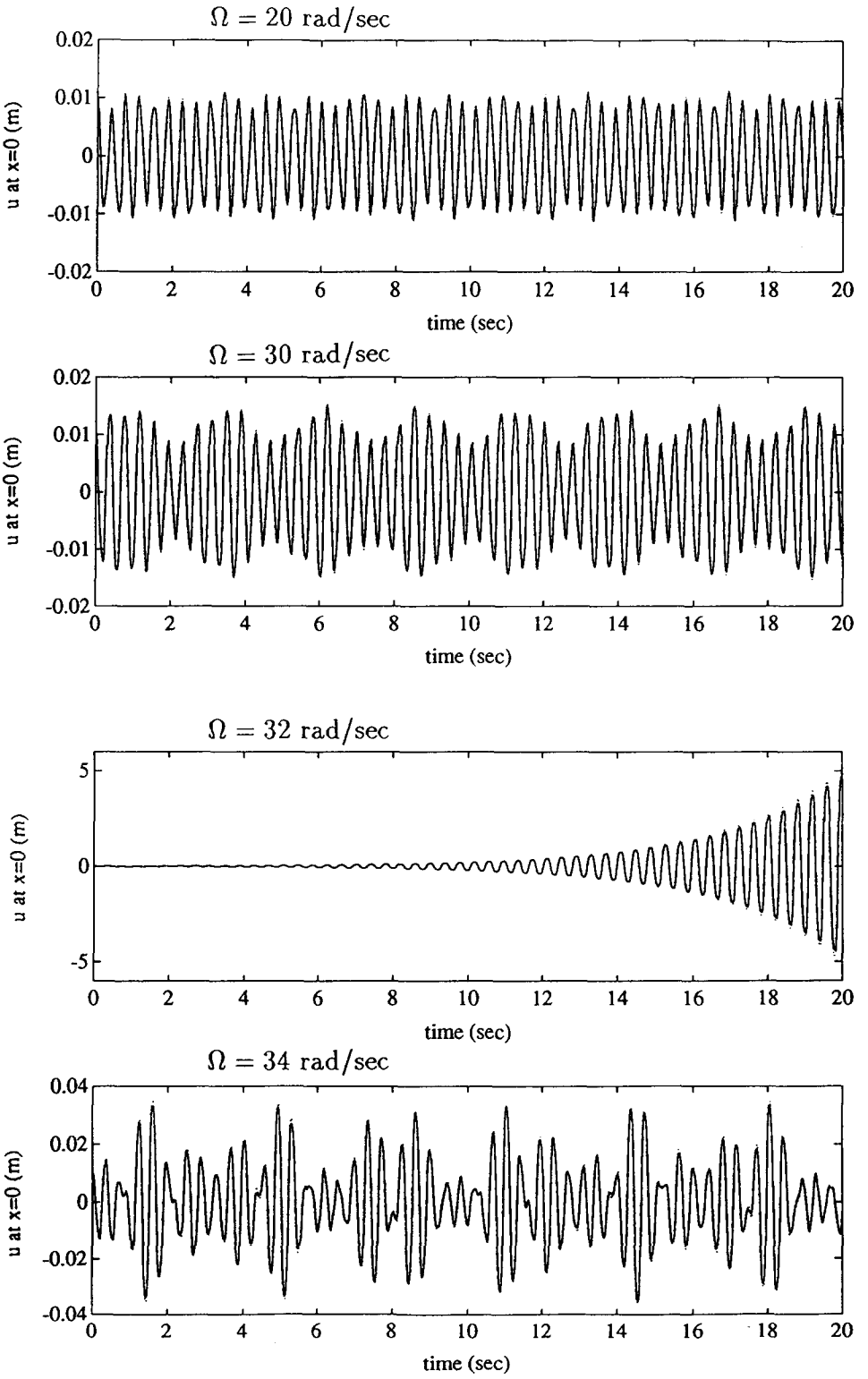

Fig. 5. Point displacements at the left edge of the plate shown in Fig. 1. Initial shape of the plate given by eqn (32): $x = 0$, $y = 0.5$ m, ———; $x = 0$, $y = 0$ m, · · ·; $x = 0$, $y = 1$ m, - - -.

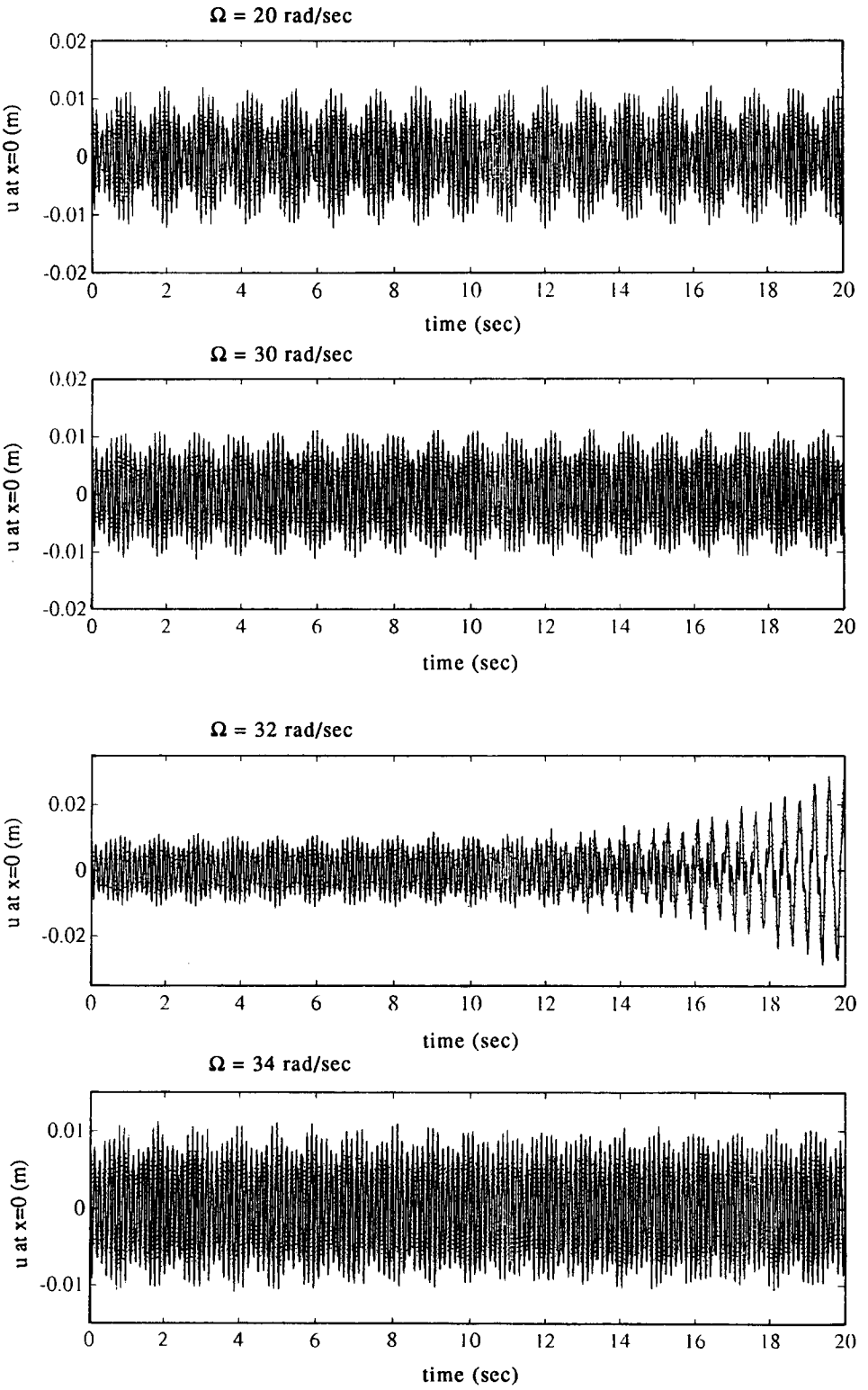

Fig. 6. Point displacements at the left edge of the plate shown in Fig. 1. Initial shape of the plate given by eqn (34): $x = 0$, $y = 0.5$ m, ———; $x = 0$, $y = 0$ m, · · ·; $x = 0$, $y = 1$ m, - - -.

are presented in Figs 7 and 8. As the supports are symmetrically located with the symmetric prescribed symmetric shape in the j direction, the point displacements at the two corners of the left edge of the plate are found to be identical at all times. However, the point displacement at the center of the left edge, shown in Fig. 7, is no longer the same as the

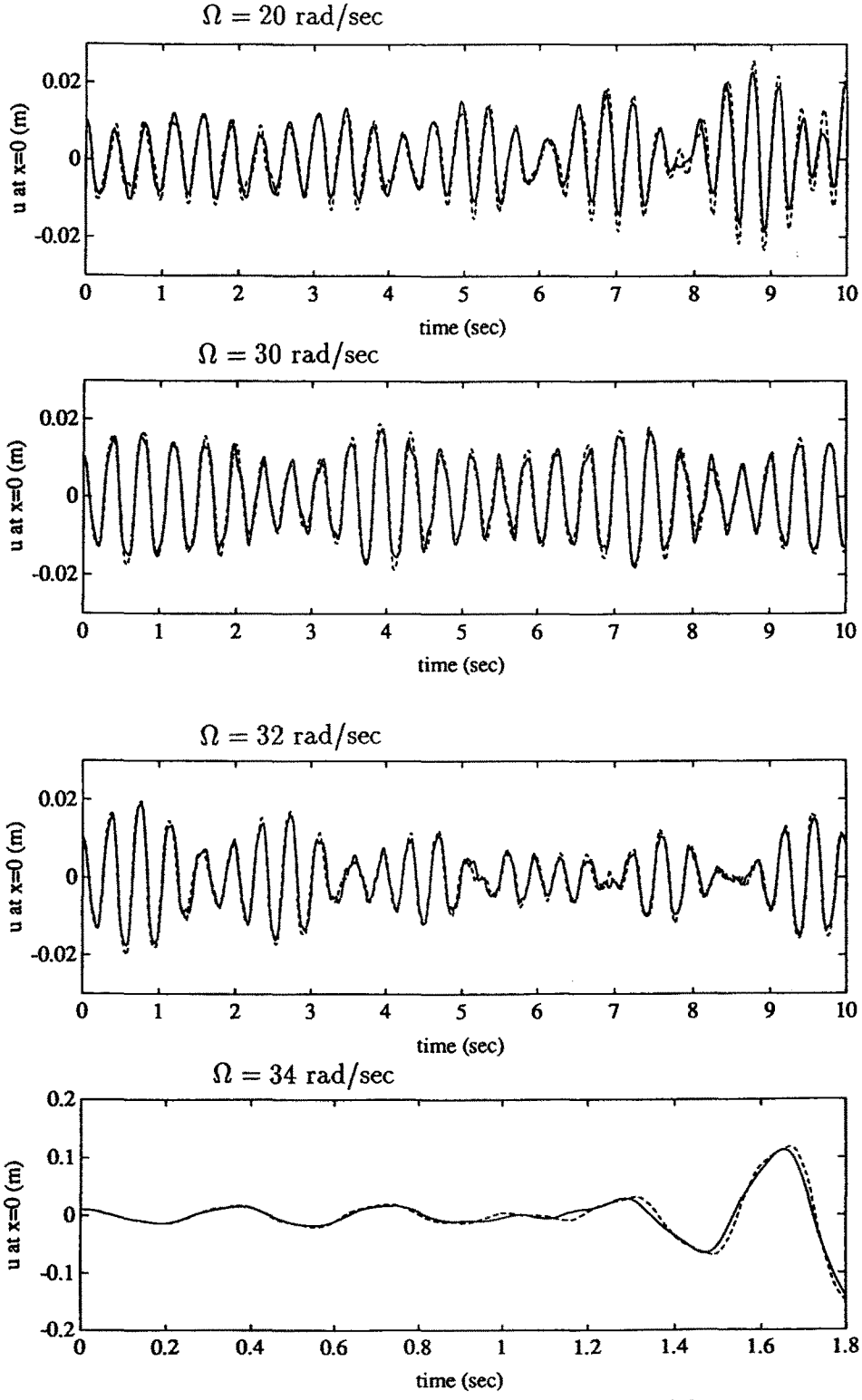

Fig. 7. Point displacements at the left edge of the plate shown in Fig. 2 with $b_1 = c_1 = 0.25$ m, $b_2 = c_2 = 0.75$ m. Initial shape of the plate given by eqn (32): $x = 0$, $y = 0.5$ m, ———; $x = 0$, $y = 0$ m, · · ·; $x = 0$, $y = 1$ m, - - -.

point displacements at the two corners of the edge although only φ_1, corresponding to the rigid body translation in the **j** direction, is prescribed for the initial shape for the motions in Fig. 7. It implies that contributions to u from terms involving $\varphi_2(y)$ to $\varphi_5(y)$ are no longer negligible. The plate appears to be unstable at $\Omega = 34$ rad s^{-1} for both of the two

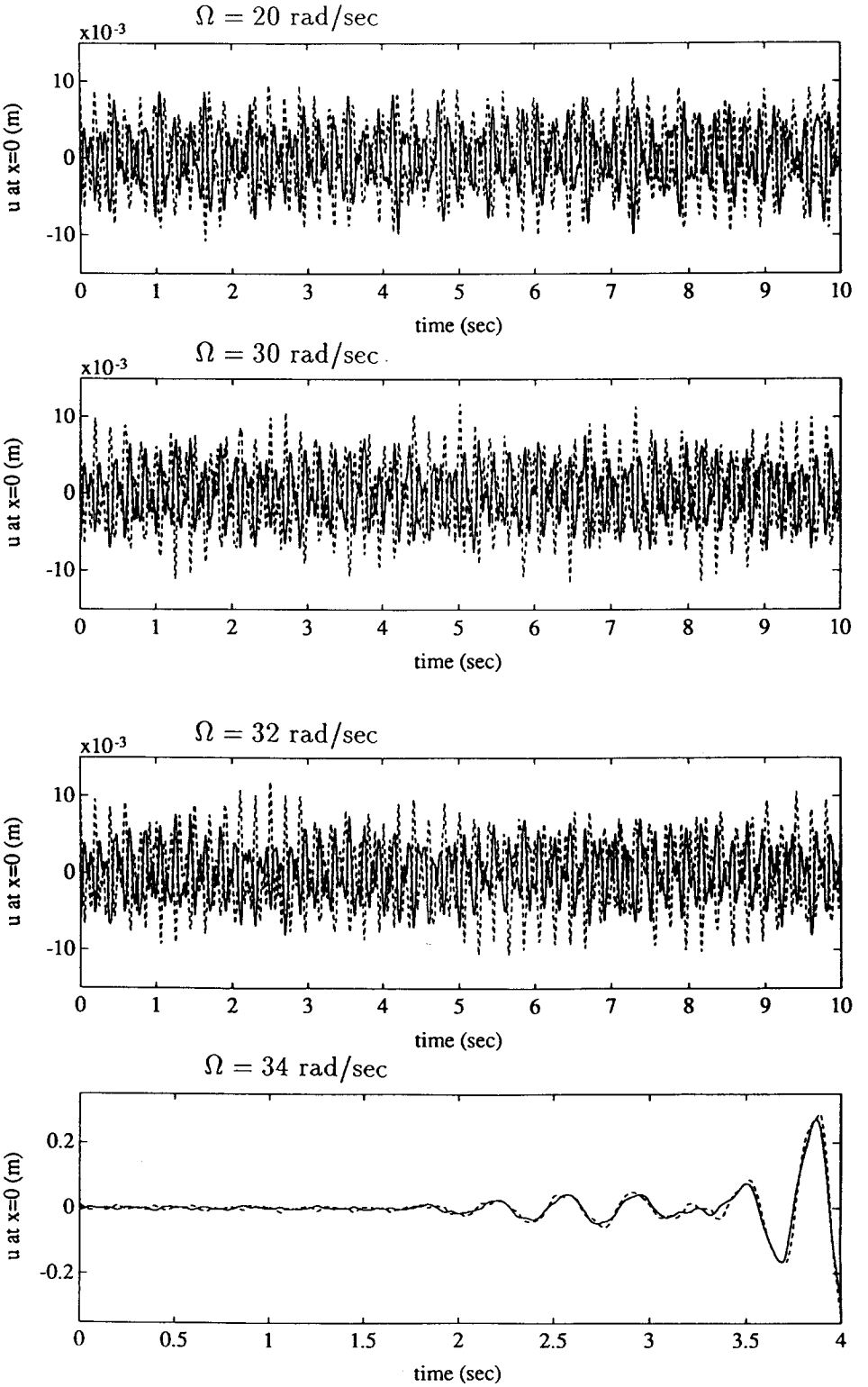

Fig. 8. Point displacements at the left edge of the plate shown in Fig. 2 with $b_1 = c_1 = 0.25$ m, $b_2 = c_2 = 0.75$ m. Initial shape of the plate given by eqn (34): $x = 0$, $y = 0.5$ m, ———; $x = 0$, $y = 0$ m, ···; $x = 0$, $y = 1$ m, - - -.

prescribed initial shapes, consistent with the fact that the stability due to the parametric excitation of a plate is not dependent on initial conditions. These stability behaviors are different, however, from the corresponding behaviors presented in Figs 5 and 6 for a plate with full-span line supports.

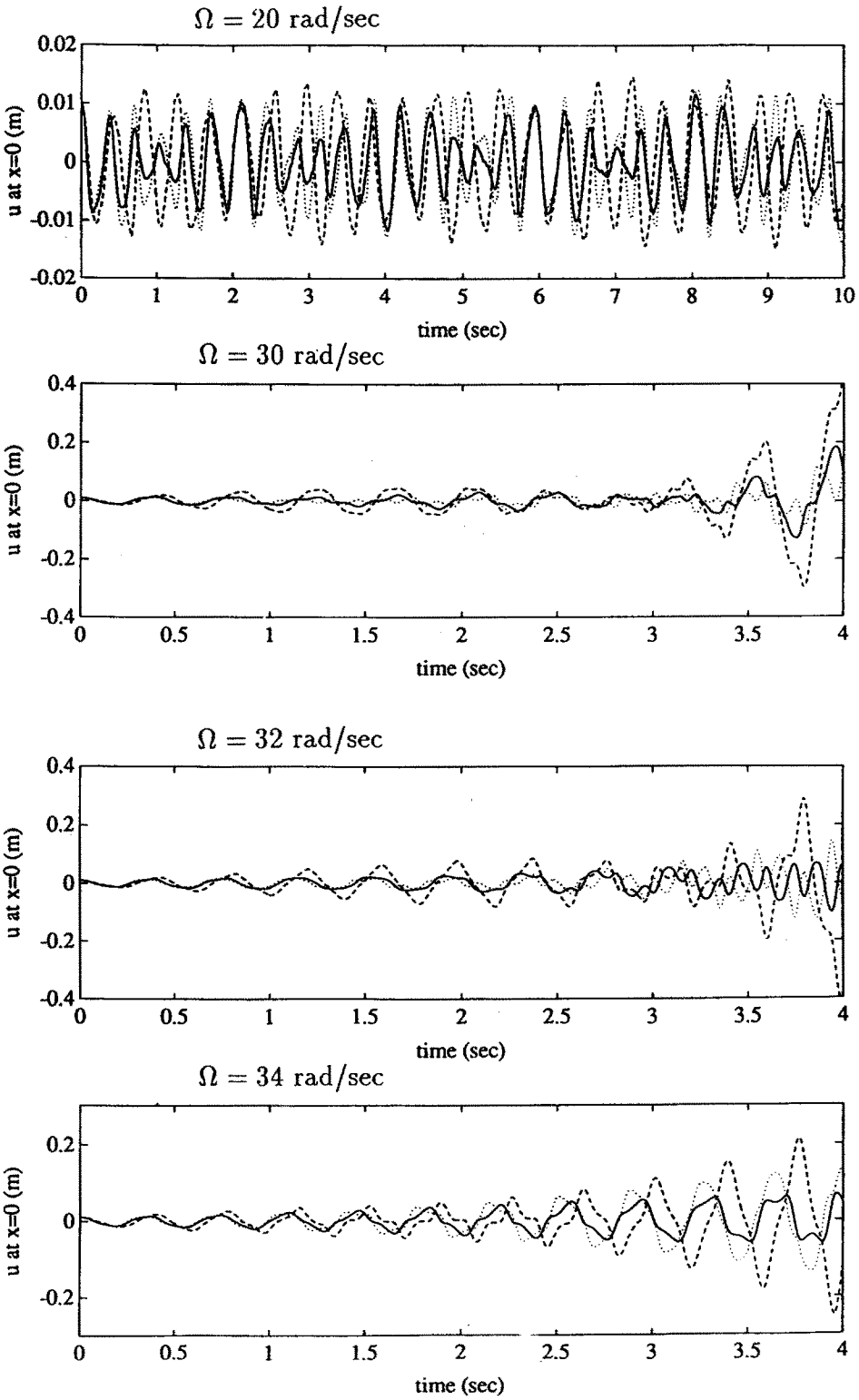

Fig. 9. Point displacements at the left edge of the plate shown in Fig. 2 with $b_1 = c_1 = 0.1$ m, $b_2 = c_2 = 0.6$ m. Initial shape of the plate given by eqn (32): $x = 0, y = 0.5$ m, ———, $x = 0, y = 0$ m, ···; $x = 0, y = 1$ m, - - -.

Numerical results for two unsymmetrically located line supports, shown in Fig. 2 with $b_1 = c_1 = 0.1$ m and $b_2 = c_2 = 0.6$ m, are presented in Figs 9 and 10 for the two different prescribed initial shapes of the plate described by eqns (32) and (34). As the supports are not symmetrically located, there are significant differences among the point displacements

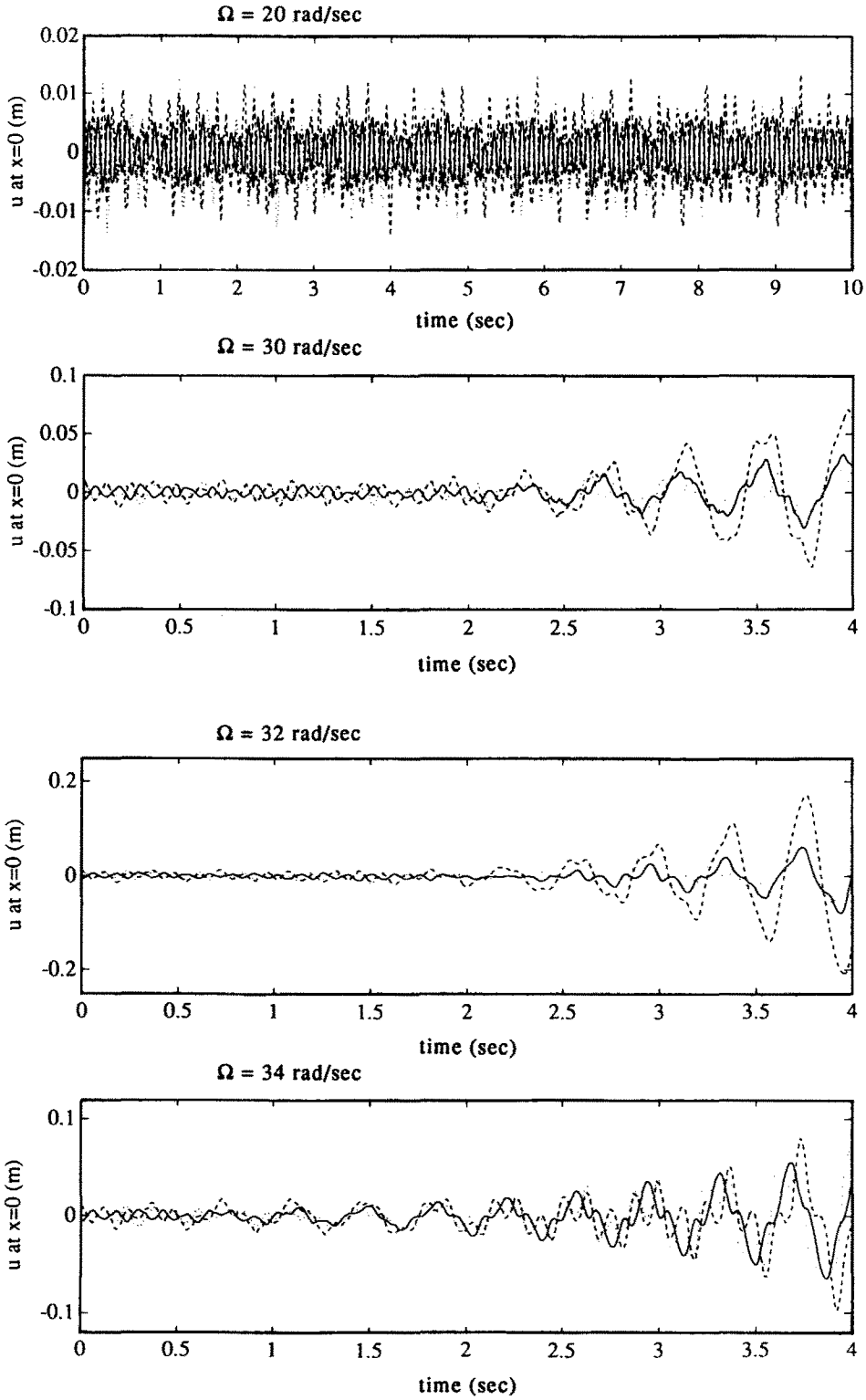

Fig. 10. Point displacements at the left edge of the plate shown in Fig. 2 with $b_1 = c_1 = 0.1$ m, $b_2 = c_2 = 0.6$ m. Initial shape of the plate given by eqn (34): $x = 0$, $y = 0.5$ m, ———; $x = 0$, $y = 0$ m, ···; $x = 0$, $y = 1$ m, - - -.

at the center and at the two corners of the left edge of the plate. Moreover, the stability behaviors are different from the preceding behaviors of a plate with symmetrically located full-span or half-span line supports.

4. CONCLUSION

Approximate equations of motion in matrix form are derived for the motion of a plate moving over multiple line supports using Hamilton's principle and the assumed mode method. The external forces that cause the motion of the plate are caused by external forces applied at one end of the plate. For in-plane sinusoidal excitation of the plate with a prescribed amplitude of excitation over the line supports, the stability of the plate is found to be dependent on the frequency of excitation and the support configuration. The behavior of a plate with arbitrarily located line supports or point supports could be easily predicted using the present formulation.

REFERENCES

Banerjee, A. K. and Kane, T. R. (1989). Dynamics of a plate in large overall motion. Trans. ASME, *J. appl. Mech.* **56,** 887–891.

Beal, T. R. (1965). Dynamic stability of a flexible missile under constant and pulsating thrusts. *J. AIAA* **56,** 887–891.

Buffinton, K. W. (1990). Parametric excitation of beams moving over supports. *Nonlinear Dyn.* **1,** 359–377.

Buffinton, K. W. (1992). Dynamics of elastic manipulators with prismatic joints. Trans. ASME, *J. dyn Syst. Meas. Control* **114,** 41–49.

Buffinton, K. W. and Kane, T. R. (1985). Dynamics of a beam moving over supports. *Int. J. Solids Struct.* **21,** 617–643.

Frýba, L. (1972). *Vibration of Solids and Structures Under Moving Loads.* Noordhoff, Groningen.

Gbadeyan, J. A. and Oni, S. T. (1992). Dynamic response to moving concentrated masses of elastic plates on a non-Winkler elastic foundation. *J. Sound Vibration* **154,** 343–358.

Lee, H. P. (1993). Dynamics of a beam moving over multiple supports. *Int. J. Solids Struct.* **30,** 199–209.

Leissa, A. W. and Co, C. M. (1984). Coriolis effects on the vibrations of rotating beams and plates. *Proc. 12th Southeastern Conf. Theoretical and Applied Mechanics*, 508–513.

Nayfeh, A. H. and Mook, D. T. (1979). *Nonlinear Oscillations.* Wiley, New York.

Raske, T. F. and Schlack, A. L. (1967). Dynamic response of plates due to moving loads. *J. Acoustical Soc. Am.* **42,** 625–635.

Stanisic, M. M., Hardin, J. C. and Lou, Y. C. (1968). On the response of a plate to a multi-masses moving system. *Acta Mech.* **5,** 37–53.

Storch, J. and Gates, S. (1985). Transverse vibration and buckling of a cantilevered beam with tip body under axial acceleration. *J. Sound Vibration* **99,** 43–52.

Young, T. H. and Liou, G. T. (1992). Coriolis effect on the vibration of a cantilever plate with time-varying rotating speed. Trans. ASME, *J. Vibration Acoustics* **114,** 232–241.

Wu, J. S., Lee, M. L. and Lai, T. S. (1987). The dynamic analysis of a flat plate under a moving load by the finite element method. *Int. J. Numer. Methods Engng* **24,** 734–762.